

Detecting dilute axion stars constrained by fast radio bursts in the solar system via stimulated decay

Haoran Di,^{1,*} Zhu Yi,^{2,3} Haihao Shi,^{4,5} and Yungui Gong^{6,†}

¹*School of Science, East China University of Technology, Nanchang 330013, China*

²*Faculty of Arts and Sciences, Beijing Normal University, Zhuhai 519087, China*

³*Advanced Institute of Natural Sciences, Beijing Normal University, Zhuhai 519087, China*

⁴*Xinjiang Astronomical Observatory, CAS, Urumqi 830011, China*

⁵*College of Astronomy and Space Science, University of Chinese Academy of Sciences, Beijing 101408, China*

⁶*Institute of Fundamental Physics and Quantum Technology, Department of Physics, School of Physical Science and Technology, Ningbo University, Ningbo 315211, China*

Fast radio bursts (FRBs) can be explained by collapsing axion stars, imposing constraints on the axion parameter space and providing valuable guidance for experimental axion searches. In the traditional post-inflationary model, axion stars could constitute up to 75% of the dark matter component, suggesting that some axion stars may exist within the solar system. Electromagnetic radiation with an angular frequency equal to half the axion mass can stimulate axion decay. Thus, directing a powerful radio beam at an axion star could trigger its stimulated decay, producing a detectable echo. Using this method, we find it is possible to test the existence of dilute axion stars with maximum masses ranging from $6.21 \times 10^{-12} M_{\odot}$ to $2.61 \times 10^{-10} M_{\odot}$, as constrained by FRBs, within the solar system. The resulting echo from axion stars constrained by FRBs could be detectable by terrestrial telescopes. Detecting such an echo would confirm the existence of axion stars, unravel the mystery of dark matter, and provide key evidence that some FRBs originate from collapsing axion stars. Furthermore, FRBs produced by axion star collapses could serve as standard candles, aiding in the resolution of the Hubble tension. If no echo is detected using this method, it would place constraints on the abundance of dark matter in the form of dilute axion stars with maximum masses in the range of $6.21 \times 10^{-12} M_{\odot}$ to $2.61 \times 10^{-10} M_{\odot}$.

I. INTRODUCTION

Growing evidence from various observations and theoretical frameworks has established that dark matter constitutes a substantial portion of the Universe’s energy density. Nonetheless, its exact nature remains elusive. The QCD axion [1, 2], arising from the Peccei-Quinn mechanism [3, 4] developed to resolve the strong CP problem, is a well-motivated candidate for dark matter. Additionally, string theory predicts a spectrum of axion-like particles (ALPs) across a wide mass range, a concept often referred to as the “axiverse” [5]. In this article, we use the term “axions” to encompass both QCD axions and ALPs. Axions can be produced through several mechanisms, such as the misalignment mechanism [6–8], the decay of string defects [9], and the kinetic misalignment mechanism [10]. Due to their bosonic nature, axions can achieve extremely high phase space densities, leading to Bose-Einstein condensation (BEC) [11] and the formation of gravitationally bound structures known as axion stars. For recent reviews, see Refs. [12–14].

The unusual orbits of trans-Neptunian objects (TNOs) [15–17] and the gravitational anomalies detected by the Optical Gravitational Lensing Experiment (OGLE) [18] remain unexplained. One potential explanation is the existence of primordial black holes (PBHs) [19] or axion stars [20] with masses in the range of $M \sim 0.5 - 20 M_{\oplus}$,

which could account for the OGLE observations. To address the TNO orbital anomalies, the planet 9 hypothesis proposes an object with a mass of $5-15 M_{\oplus}$ (approximately $1.5-4.5 \times 10^{-5} M_{\odot}$) located 300-1000 AU from the Sun [21]. A compelling possibility is that planet 9 might actually be a PBH [22] or an axion star [23] captured by the solar system. Collapsing axion stars with specific parameters may emit millisecond-long radio bursts with peak luminosities of 1.60×10^{42} erg/s, which align with the characteristics of observed non-repeating fast radio bursts (FRBs) [24]. These collapsing axion stars could serve as novel standard candles [25] for constraining the Hubble constant, H_0 , due to their strong, intrinsic luminosity being fixed and dependent solely on the axion mass and decay constant. If some FRBs are indeed produced by collapsing axion stars, this would impose constraints on the axion parameter space [25], providing valuable guidance for experimental searches for axions. Thus, exploring the axion parameter space in relation to FRBs is crucial, as it offers insight into the origin of FRBs and the nature of dark matter.

Electromagnetic radiation with an angular frequency half the axion mass can stimulate the decay of axions, producing a detectable echo. This phenomenon offers a novel opportunity to search for axion dark matter. By emitting a powerful beam of microwave radiation into space and detecting the resulting echo, axion dark matter may be identified and studied [26–30]. In our previous work, we proposed that the stimulated decay [24, 31–33] of a dilute axion star associated with planet 9 could be triggered by directing a powerful radio beam at the star,

* Corresponding author: hrdi@ecut.edu.cn

† Corresponding author: gongyungui@nbu.edu.cn

resulting in an echo detectable by terrestrial telescopes [34]. Such an observation would distinguish a dilute axion star from other planet 9 candidates, such as a PBH or a free-floating planet captured by the solar system [34]. This method offers a promising avenue for exploring the axion parameter space constrained by FRBs.

This paper is organized as follows. In Sec. II, we briefly introduce the concept of dilute axion stars. In Sec. III, we review the constraints on the axion parameter space imposed by FRBs. Section IV discusses the abundance of dilute axion stars in the Universe. In Sec. V, we analyze the potential for detecting echoes from dilute axion stars, as constrained by FRBs, within the solar system by emitting powerful radio waves into these stars. Finally, Sec. VI presents our conclusions. Throughout this article, we use natural units, where $c = \hbar = 1$.

II. DILUTE AXION STARS

The QCD axion is a hypothetical pseudo-Nambu-Goldstone boson with spin-0, characterized by a small mass m_ϕ , weak self-interactions, and extremely weak couplings to Standard Model particles. The invariance of the axion Lagrangian under the shift symmetry $\phi(x) \rightarrow \phi(x) + 2\pi f_a$ requires the axion potential $V(\phi)$ to be periodic, such that $V(\phi) = V(\phi + 2\pi f_a)$, where f_a is the axion decay constant, representing the energy scale at which the $U(1)_{\text{PQ}}$ symmetry spontaneously breaks. Performing a series expansion of the axion potential around $\phi = 0$, considering only the first two leading terms, the potential can be expressed as

$$V(\phi) = \frac{1}{2} m_\phi^2 \phi^2 + \frac{\lambda}{4!} \phi^4 + \mathcal{O}\left(\frac{\lambda^2 \phi^6}{6! m_\phi^2}\right), \quad (1)$$

where $\lambda = -\kappa m_\phi^2 / f_a^2$ represents the attractive self-interaction coupling constant. The value of κ depends on the choice of axion potential. For the instanton potential, $V(\phi) = (m_\phi f_a)^2 [1 - \cos(\phi/f_a)]$, commonly used in axion phenomenology, $\kappa = 1$. For the chiral potential [35, 36], $\kappa \simeq 0.34$ [36, 37]. Considering the interaction between axions and photons, the general Lagrangian for the axion is given by

$$\begin{aligned} \mathcal{L} = & \frac{1}{2} \partial_\mu \phi \partial^\mu \phi - \frac{1}{2} m_\phi^2 \phi^2 - \frac{\lambda}{4!} \phi^4 - \mathcal{O}\left(\frac{\lambda^2 \phi^6}{6! m_\phi^2}\right) \\ & + \frac{\alpha K}{8\pi f_a} \phi F_{\mu\nu} \tilde{F}^{\mu\nu} - \frac{1}{4} F_{\mu\nu} F^{\mu\nu}, \end{aligned} \quad (2)$$

where $F_{\mu\nu}$ is the electromagnetic field strength tensor, $\tilde{F}^{\mu\nu}$ is its dual, α is the fine-structure constant, and K is a model-dependent constant of order one. Axions are not entirely stable and can decay into two photons via the interaction term $\mathcal{L}_{int} = \frac{\alpha K}{8\pi f_a} \phi F_{\mu\nu} \tilde{F}^{\mu\nu}$. This interaction has significant astrophysical implications and provides an experimental window for the search for these elusive particles. The decay rate of an axion at rest into two photons

is

$$\begin{aligned} \Gamma_\phi &= \frac{\alpha^2 K^2 m_\phi^3}{256\pi^3 f_a^2} \\ &= 1.02 \times 10^{-50} \text{ s}^{-1} K^2 \left(\frac{m_\phi}{10^{-5} \text{ eV}}\right)^3 \left(\frac{f_a}{10^{12} \text{ GeV}}\right)^{-2}. \end{aligned} \quad (3)$$

For QCD axions, there exists a well-known relationship between the decay constant f_a and the axion mass [1]:

$$\begin{aligned} m_\phi &= \frac{\sqrt{m_u m_d} f_\pi m_\pi}{m_u + m_d f_a} \\ &\simeq 6 \times 10^{-6} \text{ eV} \left(\frac{f_a}{10^{12} \text{ GeV}}\right)^{-1}, \end{aligned} \quad (4)$$

where $m_u \simeq 2.2$ MeV, $m_d \simeq 4.7$ MeV, and $m_\pi \simeq 135$ MeV are the masses of the up quark, down quark, and pion, respectively, while $f_\pi \simeq 92$ MeV is the pion decay constant. This relationship is illustrated in Fig. 1. As bosons, axions can achieve exceptionally high phase space densities, potentially leading to the formation of BECs [11]. These BECs can result in axion stars, which may manifest in both dilute and dense configurations [38–40]. However, dense axion stars may have lifespans too short to significantly impact cosmology as astrophysical objects [12, 41–44].

A stable dilute axion star is in equilibrium, where the attractive forces of self-gravity and self-interactions are balanced by the repulsive gradient energy. This equilibrium is maintained as long as the star's density remains low, thereby minimizing the effects of self-interactions. However, if the mass of the dilute axion star exceeds a critical threshold, determined by the attractive self-interaction coupling constant, this equilibrium becomes disrupted. The maximum mass and corresponding minimum radius of a dilute axion star are given by [45, 46]

$$M_{\text{max}} \sim 5.073 \frac{M_{pl}}{\sqrt{|\lambda|}}, \quad R_{\text{min}} \sim \sqrt{|\lambda|} \frac{M_{pl}}{m_\phi} \lambda_c, \quad (5)$$

where M_{pl} is the Planck mass and λ_c denotes the Compton wavelength of the axion. When the mass of a dilute axion star exceeds the critical mass given by Eq. (5), either due to merger events [47–53] or through the accretion of axions from the surrounding environment [54–56], self-interactions become significant, potentially leading to the collapse of the star [57–59]. Substituting the attractive coupling constant of self-interaction, $\lambda = -\kappa m_\phi^2 / f_a^2$, and the axion's Compton wavelength, $\lambda_c = 2\pi / m_\phi$, into Eq. (5), the critical mass and minimum radius are expressed as

$$\begin{aligned} M_{\text{max}} &\sim 5.97 \times 10^{-12} M_\odot \kappa^{-1/2} \\ &\times \left(\frac{m_\phi}{10^{-5} \text{ eV}}\right)^{-1} \left(\frac{f_a}{10^{12} \text{ GeV}}\right), \end{aligned} \quad (6)$$

$$\begin{aligned} R_{\text{min}} &\sim 2.41 \times 10^2 \text{ km} \kappa^{1/2} \\ &\times \left(\frac{m_\phi}{10^{-5} \text{ eV}}\right)^{-1} \left(\frac{f_a}{10^{12} \text{ GeV}}\right)^{-1}. \end{aligned} \quad (7)$$

These quantities depend not only on the mass and decay constant of the axion but also on the choice of axion potential. For a general dilute axion star, we denote its mass as M_{AS} and its radius as R_{AS} .

III. CONSTRAINTS BY FAST RADIO BURSTS

Since the axion is a pseudoscalar boson, the boson enhancement effect must be considered. The change in photon number density $n_{\lambda'}$ within the dilute axion star is governed by the Boltzmann equation [31]:

$$\begin{aligned} \frac{dn_{\lambda'}}{dt} = & \int dX_{LIPS} |\mathcal{M}(\phi \rightarrow \gamma(\lambda')\gamma(\lambda'))|^2 \\ & \times \{f_{\phi}(\mathbf{p})[1 + f_{\lambda'}(\mathbf{k}_1)][1 + f_{\lambda'}(\mathbf{k}_2)] \\ & - f_{\lambda'}(\mathbf{k}_1)f_{\lambda'}(\mathbf{k}_2)[1 + f_{\phi}(\mathbf{p})]\}, \end{aligned} \quad (8)$$

where f_{ϕ} and $f_{\lambda'}$ represent the phase space densities of the axion and photon, respectively. The term $\mathcal{M}(\phi \rightarrow \gamma(\lambda')\gamma(\lambda'))$ refers to the matrix element corresponding to the interaction $\mathcal{L}_{\text{int}} = \frac{\alpha K}{8\pi f_a} \phi F_{\mu\nu} \tilde{F}^{\mu\nu}$. The phase space integration is performed using the standard Lorentz-invariant measure, considering the momenta of both the axion and the photons. Assuming the phase space distributions of axions and photons are approximately uniform and isotropic within the dilute axion star, the time evolution of photon number density becomes [31, 32]

$$\frac{dn_{\gamma}}{dt} = \Gamma_{\phi} \left[2n_{\phi} \left(1 + \frac{8\pi^2}{m_{\phi}^3 v} n_{\gamma} \right) - \frac{16\pi^2}{3m_{\phi}^3} \left(v + \frac{3}{2} \right) n_{\gamma}^2 \right], \quad (9)$$

where $v \sim 1/(2R_{AS}m_{\phi})$ represents the maximum axion velocity within the dilute axion star, as estimated using the Heisenberg uncertainty principle.

In Eq. (9), the initial terms within the square brackets represent both spontaneous and stimulated decay. The final term, scaled by a factor of 3/2, corresponds to the production of “sterile” axions [31], which can escape from the dilute axion star. Furthermore, photons produced through spontaneous and stimulated decay escape from the dilute axion star at a rate of $\Gamma_e = 1/R_{AS}$. By integrating Eq. (9) and accounting for the escaped photons, the coupled differential equations describing the evolution of the number of axions and photons within the dilute axion star are expressed as follows [25]

$$\begin{aligned} \frac{dN_{\gamma}}{dt} = & 2\Gamma_{\phi}N_{\phi} + \frac{12\pi}{m_{\phi}^3 v R_{AS}^3} \Gamma_{\phi}N_{\phi}N_{\gamma} \\ & - \frac{2\pi(2v+3)}{m_{\phi}^3 R_{AS}^3} \Gamma_{\phi}N_{\gamma}^2 - \Gamma_e N_{\gamma}, \end{aligned} \quad (10)$$

$$\begin{aligned} \frac{dN_{\phi}}{dt} = & -\Gamma_{\phi}N_{\phi} - \frac{6\pi}{m_{\phi}^3 v R_{AS}^3} \Gamma_{\phi}N_{\phi}N_{\gamma} \\ & + \frac{4\pi v}{m_{\phi}^3 R_{AS}^3} \Gamma_{\phi}N_{\gamma}^2. \end{aligned} \quad (11)$$

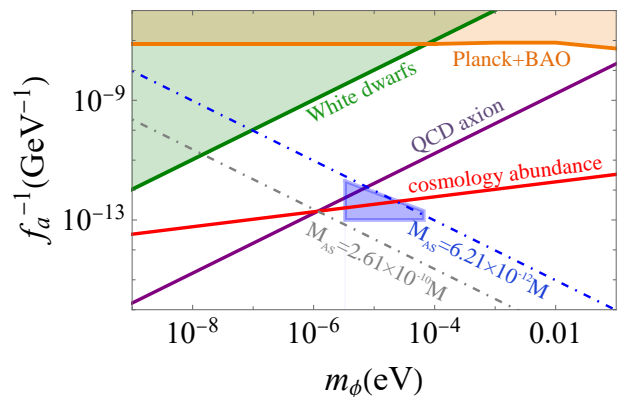


FIG. 1. The parameter space of axions. The region above the orange solid line is excluded based on constraints from Planck 2018 combined with BAO measurements [60]. Constraints derived from white dwarf observations are represented by the green area [61], with the latest findings detailed in Ref. [62]. The purple line corresponds to QCD axions, while the blue region represents the parameter space constrained by FRBs, where the maximum mass of dilute axion stars ranges from $6.21 \times 10^{-12} M_{\odot}$ to $2.61 \times 10^{-10} M_{\odot}$.

However, even for dilute axion stars in a critical state, the photon number $N_{\gamma} \simeq (2\Gamma_{\phi}/\Gamma_e)N_{\phi}$ resulting from spontaneous decay is insufficient to initiate stimulated decay.

When the axion star mass exceeds the critical threshold, it collapses. As the size approaches the critical radius $R_{cr} \simeq 24\pi\Gamma_{\phi}M_{\text{max}}/m_{\phi}^3$ [25], stimulated decay initiates. The luminosity of the collapsing axion star from stimulated decay is given by [25]

$$\begin{aligned} L_{\phi} = & \frac{1}{2}m_{\phi}N_{\gamma}R_{cr}^{-1} = \frac{N_{\gamma}m_{\phi}^4}{48\pi\Gamma_{\phi}M_{\text{max}}} \\ \sim & 3.60 \times 10^{40} \text{erg/s} \left(\frac{N_{\gamma}}{10^{49}} \right) \left(\frac{m_{\phi}}{10^{-5} \text{eV}} \right)^2 \left(\frac{f_a}{10^{12} \text{GeV}} \right), \end{aligned} \quad (12)$$

where model-dependent constants $K = 1$ and $\kappa = 1$ are assumed. Detection of a radio signal consistent with the stimulated decay of a collapsing axion star could serve as a standard candle for constraining the Hubble constant, given the intense luminosity of such a radio burst [25].

Interestingly, radio signals from the stimulated decay of collapsing axion stars may already have been detected. FRBs are bright, transient radio emissions lasting only milliseconds [63–65], with a frequency range spanning approximately 400 MHz to 8 GHz [66] and total energy outputs typically between 10^{38} and 10^{40} erg [65, 67]. The photon frequency and total energy emitted by a collapsing axion star, for certain parameter ranges, align with those observed in FRBs [25]. For constraints on the axion parameter space derived from FRBs, see Ref. [25] and Fig. 1. The maximum axion star mass within this constrained parameter space ranges from approximately

$6.21 \times 10^{-12} M_\odot$ to $2.61 \times 10^{-10} M_\odot$, as shown in Fig. 1.

IV. ABUNDANCE OF DILUTE AXION STARS

The current relic density of axions is described by the equation [23]:

$$\Omega_\phi h^2 \simeq 0.12 \left(\frac{g_*(T_{\text{osc}})}{106.75} \right)^{3/4} \left(\frac{m_\phi}{10^{-6} \text{ eV}} \right)^{1/2} \times \left(\frac{f_a}{5.32 \times 10^{12} \text{ GeV}} \right)^2. \quad (13)$$

This equation, applicable to axions produced via the misalignment mechanism, defines the lower bound of the axion parameter space, as shown in Fig. 1. By combining Eq. (4) with Eq. (13), we obtain the axion mass $m_\phi \simeq 1.17 \times 10^{-6} \text{ eV}$ and the decay constant $f_a \simeq 5.11 \times 10^{12} \text{ GeV}$, under the assumption that QCD axions constitute the majority of dark matter. Substituting these values into Eq. (6), the maximum mass of the corresponding dilute axion star is calculated to be approximately $2.61 \times 10^{-10} M_\odot$. This value coincides with the upper limit of the maximum axion star mass constrained by the parameter space derived from FRBs, as shown in Fig. 1. From Fig. 1, it is evident that the cosmological abundance line intersects the parameter space constrained by FRBs. This overlap significantly enhances the likelihood of axions existing within this region and provides additional support for the misalignment mechanism as a potential source of axions.

In the standard post-inflationary scenario, where $U(1)_{\text{PQ}}$ symmetry is spontaneously broken after inflation, axion overdensities collapse during the radiation-dominated epoch, forming an early population of miniclusters with masses up to $10^{-12} M_\odot$ [68–70]. By redshift $z = 100$, about 75% of axion dark matter resides within these bound structures [71], with minicluster masses reaching up to $10^{-9} M_\odot$ due to mergers. This closely matches the mass range of $6.21 \times 10^{-12} M_\odot$ to $2.61 \times 10^{-10} M_\odot$ for axion stars constrained by FRBs. Dilute axion stars evolve toward a critical state through the accretion of axions from the surrounding environment or via merger events. Once they surpass this critical threshold, they collapse, emitting strong radio signals [24] or relativistic axions [57]. After the collapse, a residual dilute axion star remains, retaining a mass close to its critical value and entering a subcritical state. This suggests that the likelihood of dilute axion stars being in either a critical or subcritical state is relatively high. For simplicity, we will assume that dilute axion stars are in a critical state in the following discussion.

The local dark matter density ρ_{DM} near the solar system is estimated to be $0.01 M_\odot \text{ pc}^{-3} \approx 0.4 \text{ GeV/cm}^3$, as inferred from stellar dynamics on scales greater than approximately 100 parsecs [72–75]. Using this value, the local number density of dilute axion stars can be calcu-

lated as:

$$n_{\text{AS}} = \frac{\Omega_{\text{AS}} \rho_{\text{DM}}}{\Omega_{\text{DM}} M_{\text{AS}}} \quad (14)$$

$$= 1.27 \times 10^9 \text{ pc}^{-3} \left(\frac{\Omega_{\text{AS}}}{0.75 \Omega_{\text{DM}}} \right) \left(\frac{6.21 \times 10^{-12} M_\odot}{M_{\text{AS}}} \right),$$

where $\Omega_{\text{AS}}/\Omega_{\text{DM}}$ represents the fraction of dilute axion stars within dark matter. Assuming 75% of dark matter is composed of axion stars, a spherical volume with a radius of 1000 AU would contain approximately 605 axion stars with a mass of $6.21 \times 10^{-12} M_\odot$, or 14 axion stars with a mass of $2.61 \times 10^{-10} M_\odot$. The number density of dilute axion stars is inversely proportional to their mass: lower-mass axion stars are more numerous, increasing their likelihood of being present in the solar system. This suggests that low-mass dilute axion stars, with maximum masses ranging from $6.21 \times 10^{-12} M_\odot$ to $2.61 \times 10^{-10} M_\odot$, could potentially be detected within the solar system.

V. ECHO FROM DILUTE AXION STARS

A dilute axion star remains stable because the photon number resulting from spontaneous decay is insufficient to initiate stimulated decay. Now, consider transmitting radio waves with power P to a dilute axion star. The coupled differential equations describing the evolution of the number of axions and photons within the dilute axion star are then modified as follows:

$$\frac{dN_\gamma}{dt} = 2\Gamma_\phi N_\phi + \frac{12\pi}{m_\phi^3 v R_{\text{AS}}^3} \Gamma_\phi N_\phi (N_\gamma + N_{\gamma 0}) - \frac{2\pi(2v+3)}{m_\phi^3 R_{\text{AS}}^3} \Gamma_\phi (N_\gamma + N_{\gamma 0})^2 - \Gamma_e N_\gamma, \quad (15)$$

$$\frac{dN_\phi}{dt} = -\Gamma_\phi N_\phi - \frac{6\pi}{m_\phi^3 v R_{\text{AS}}^3} \Gamma_\phi N_\phi (N_\gamma + N_{\gamma 0}) + \frac{4\pi v}{m_\phi^3 R_{\text{AS}}^3} \Gamma_\phi (N_\gamma + N_{\gamma 0})^2, \quad (16)$$

where $N_{\gamma 0} \simeq 2PR_{\text{AS}}/m_\phi$ represents the number of radio wave photons emitted from Earth and transmitted into the dilute axion star. By substituting Eq. (7) with $\kappa = 1$ into $N_{\gamma 0}$, we obtain

$$N_{\gamma 0} \simeq 5.02 \times 10^{28} \left(\frac{P}{50 \text{ MW}} \right) \times \left(\frac{m_\phi}{10^{-5} \text{ eV}} \right)^{-2} \left(\frac{f_a}{10^{12} \text{ GeV}} \right)^{-1}. \quad (17)$$

Stimulated decay dominates over spontaneous decay when the condition $6\pi(N_\gamma + N_{\gamma 0})/(m_\phi^3 v R_{\text{AS}}^3) > 1$ is satisfied. By transmitting radio waves with a power of $P = 50 \text{ MW}$ into the dilute axion star, we calculate

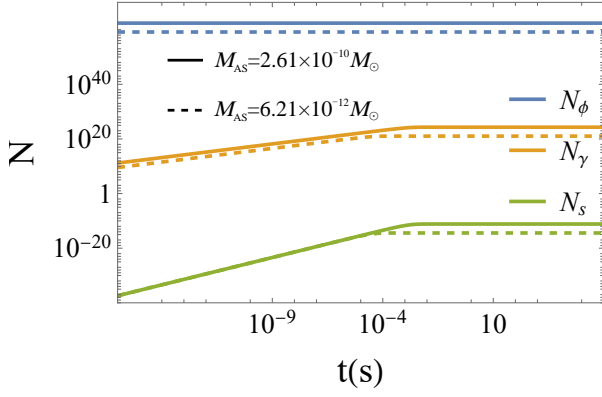


FIG. 2. Numerical evolution of the axion, photon, and “sterile” axion numbers within a dilute axion star under a powerful microwave radiation beam of 50MW. The solid line represents an axion star with a mass of $M_{AS} = 2.61 \times 10^{-10} M_{\odot}$ and parameters $m_{\phi} = 1.17 \times 10^{-6}$ eV and $f_a = 5.11 \times 10^{12}$ GeV. The dashed line corresponds to an axion star with a mass of $M_{AS} = 6.21 \times 10^{-12} M_{\odot}$ and parameters $m_{\phi} = 5 \times 10^{-5}$ eV and $f_a = 5.20 \times 10^{12}$ GeV. Timing begins when the axion star is irradiated with radio waves. For $M_{AS} = 6.21 \times 10^{-12} M_{\odot}$, the stimulated decay of the dilute axion star stabilizes after approximately 10^{-4} seconds of irradiation, with a photon number of $N_{\gamma} = 1.10 \times 10^{21}$.

$N_{\gamma 0} = 3.86 \times 10^{26}$ and find that $6\pi N_{\gamma 0} / (m_{\phi}^3 v R_{AS}^3) = 2.64 \times 10^{15} \gg 1$, using the parameters $m_{\phi} = 5 \times 10^{-5}$ eV and $f_a = 5.20 \times 10^{12}$ GeV. Thus, radio waves of sufficient power, such as $P = 50$ MW, can effectively induce the stimulated decay of a dilute axion star. The multi-beam relativistic klystron amplifier currently has the capability to generate radio waves with an output power of 1.047 GW [76], significantly exceeding the required 50 MW. This substantial power output makes it a promising candidate for emitting radio waves to interact with axion stars. In the following discussion, we will use the example of a 50 MW radio wave received by an axion star.

Figure 2 presents two numerical solutions showing the evolution of axion, photon, and “sterile” axion numbers for two representative parameter sets. The solid line corresponds to an axion star with a critical mass of $M_{AS} = 2.61 \times 10^{-10} M_{\odot}$ with parameters $m_{\phi} = 1.17 \times 10^{-6}$ eV and a decay constant $f_a = 5.11 \times 10^{12}$ GeV, representing the intersection of cosmological abundance and QCD axion constraints in Fig. 1. The dashed line corresponds to an axion star with a critical mass of $M_{AS} = 6.21 \times 10^{-12} M_{\odot}$, with parameters lying within the region constrained by FRBs: $m_{\phi} = 5 \times 10^{-5}$ eV and $f_a = 5.20 \times 10^{12}$ GeV. For the case $M_{AS} = 6.21 \times 10^{-12} M_{\odot}$, the stimulated decay of the dilute axion star stabilizes after approximately 10^{-4} seconds of irradiation, resulting in a photon number $N_{\gamma} = 1.10 \times 10^{21}$. Considering the photons escaping from the dilute axion star, the luminosity

can be expressed as:

$$L_{\phi} = \frac{1}{2} m_{\phi} N_{\gamma} \Gamma_e. \quad (18)$$

A notable feature of stimulated decay is that, in the axion rest frame, the emitted photons are restricted to propagate either in the same direction as or directly opposite to the incoming photons. However, the velocity distribution of axions within the dilute axion star introduces spatial dispersion of the emitted photons. Consequently, the luminosity flux observed from Earth is roughly given by

$$F_{\phi} \sim \frac{L_{\phi}}{4\pi d^2} = \frac{m_{\phi} N_{\gamma} \Gamma_e}{8\pi d^2}, \quad (19)$$

where d represents the distance between the dilute axion star and Earth. For a dilute axion star in its critical state, substituting Eq. (7) with $\kappa = 1$ into $\Gamma_e = R_{AS}^{-1}$, the photon escape rate becomes

$$\Gamma_e \sim 1.24 \times 10^3 \text{ s}^{-1} \left(\frac{m_{\phi}}{10^{-5} \text{ eV}} \right) \left(\frac{f_a}{10^{12} \text{ GeV}} \right). \quad (20)$$

By substituting Eq. (20) into Eq. (19), the flux can be expressed as

$$F_{\phi} = 3.50 \times 10^{-35} \left(\frac{m_{\phi}}{10^{-5} \text{ eV}} \right)^2 \left(\frac{f_a}{10^{12} \text{ GeV}} \right) \times \left(\frac{N_{\gamma}}{10^{20}} \right) \left(\frac{1000 \text{ AU}}{d} \right)^2 \text{ W/cm}^2. \quad (21)$$

As illustrated in Fig. 1, the critical mass of dilute axion stars constrained by FRBs ranges from approximately $6.21 \times 10^{-12} M_{\odot}$ to $2.61 \times 10^{-10} M_{\odot}$. Substituting Eq. (6) with $\kappa = 1$ into Eq. (21) for a mass of $6.21 \times 10^{-12} M_{\odot}$, the luminosity flux of the dilute axion star is calculated as

$$F_{\phi} = 3.64 \times 10^{-34} \left(\frac{m_{\phi}}{10^{-5} \text{ eV}} \right)^3 \times \left(\frac{N_{\gamma}}{10^{21}} \right) \left(\frac{1000 \text{ AU}}{d} \right)^2 \text{ W/cm}^2, \quad (22)$$

corresponding to the blue dot-dashed line with a flux of $F_{\phi} \approx 4.86 \times 10^{-32}$ W/cm² for $d = 1000$ AU, as shown in Fig. 3. Similarly, substituting Eq. (6) with $\kappa = 1$ into Eq. (21) for a mass of $2.61 \times 10^{-10} M_{\odot}$ gives

$$F_{\phi} = 1.53 \times 10^{-32} \left(\frac{m_{\phi}}{10^{-6} \text{ eV}} \right)^3 \times \left(\frac{N_{\gamma}}{10^{24}} \right) \left(\frac{1000 \text{ AU}}{d} \right)^2 \text{ W/cm}^2, \quad (23)$$

which corresponds to the gray line for $d = 1000$ AU, effectively overlapping with the blue dot-dashed line, as shown in Fig. 3. Therefore, the luminosity flux of the echo from dilute axion stars at a distance of 1000 AU, as observed from Earth, is approximately $4.86 \times$

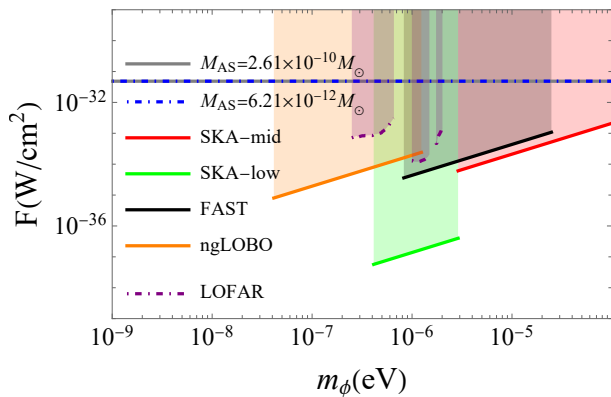


FIG. 3. Flux of the dilute axion star at a distance of 1000 AU and the minimum detectable flux of SKA, FAST, ngLOBO, and LOFAR with an observation time of 1 hour. The sensitivity of these telescopes is detailed in Ref. [34] and its references. Even for LOFAR, the flux of the echoes is one to two orders of magnitude higher than its sensitivity, making the signal easily detectable and distinguishable.

10^{-32} W/cm², corresponding to an axion star mass range of $6.21 \times 10^{-12} M_{\odot}$ to $2.61 \times 10^{-10} M_{\odot}$, as constrained by FRBs. This flux exceeds the sensitivity thresholds of radio telescopes such as SKA, FAST, ngLOBO, and LOFAR with an observation time of 1 hour, as shown in Fig. 3. Thus, the decay signal is detectable by these radio telescopes.

Consequently, the stimulated decay of a dilute axion star within a volume of radius 1000 AU centered around Earth can be triggered by emitting a 50 MW radio beam into the star. The spectral line of the decay signal is nearly monochromatic, with a frequency of $f \simeq m_{\phi}/(4\pi) \approx 1.21(m_{\phi}/10^{-5}\text{eV})$ GHz, making it a distinct characteristic signal. Detection of such an echo would confirm the existence of axion stars, solve the dark matter puzzle, and provide crucial evidence linking some FRBs to axion stars. Furthermore, FRBs originating from collapsing axion stars could serve as standard candles to help resolve the Hubble tension [25]. If such echoes are not detected within a 1000 AU volume around Earth using this method, constraints can be placed on the fraction of dark matter composed of dilute axion stars with critical masses constrained by FRBs. This fraction could be roughly less than 5% for a mass of $6.21 \times 10^{-12} M_{\odot}$ or 0.1% for a mass of $2.61 \times 10^{-10} M_{\odot}$, depending on the axion parameters. This estimate assumes a uniform distribution of axion stars throughout the Universe.

VI. CONCLUSIONS

Axions are a promising candidate for dark matter. Due to their bosonic nature, axions can achieve very high phase space densities, resulting in BEC and the formation of gravitationally bound structures known as axion stars. Collapsing axion stars with specific parameters may emit millisecond-long radio bursts with peak luminosities of 1.60×10^{42} erg/s, aligning with the characteristics of observed non-repeating FRBs. If some FRBs are indeed produced by collapsing axion stars, this would impose constraints on the axion parameter space, offering valuable guidance for experimental axion searches. Thus, exploring the axion parameter space in relation to FRBs is crucial, as it relates both to the origin of FRBs and the nature of dark matter.

In the traditional post-inflationary scenario, axion stars could account for up to 75% of dark matter, suggesting that some may exist within the solar system. Building on previous work that explored the possibility of explaining planet 9 as a dilute axion star via stimulated decay induced by a 50 MW radio beam, we propose extending this method to search for dilute axion stars with masses ranging from $6.21 \times 10^{-12} M_{\odot}$ to $2.61 \times 10^{-10} M_{\odot}$. These masses are constrained by the characteristics of FRBs, which could potentially be explained by collapsing axion stars. For axions within the parameter space constrained by FRBs, the echo resulting from the stimulated decay of axion stars could be detectable by ground-based radio telescopes. Detection of such an echo would not only confirm the existence of axion stars but also provide key evidence linking axion stars to FRBs. Furthermore, using FRBs from axion star collapses as standard candles could aid in resolving the Hubble tension. If no signal is detected, this method will provide constraints on the abundance of dark matter in the form of dilute axion stars with masses between $6.21 \times 10^{-12} M_{\odot}$ and $2.61 \times 10^{-10} M_{\odot}$. Under the assumption of a uniform distribution of dilute axion stars across the Universe, the abundance would be limited to less than approximately 5% for masses of $6.21 \times 10^{-12} M_{\odot}$ or 0.1% for masses of $2.61 \times 10^{-10} M_{\odot}$.

VII. ACKNOWLEDGMENTS

H. Di would like to thank Lijing Shao for useful discussions. This work was supported by National Natural Science Foundation of China under Grant No. 11947031 and East China University of Technology Research Foundation for Advanced Talents under Grant No. DHBK2019206.

[1] S. Weinberg, A new light boson?, *Phys. Rev. Lett.* **40**, 223 (1978).

[2] F. Wilczek, Problem of strong P and T invariance in the presence of instantons, *Phys. Rev. Lett.* **40**, 279 (1978).

- [3] R. D. Peccei and H. R. Quinn, Constraints imposed by CP conservation in the presence of pseudoparticles, *Phys. Rev. D* **16**, 1791 (1977).
- [4] R. D. Peccei and H. R. Quinn, CP conservation in the presence of pseudoparticles, *Phys. Rev. Lett.* **38**, 1440 (1977).
- [5] A. Arvanitaki, S. Dimopoulos, S. Dubovsky, N. Kaloper and J. March-Russell, String axiverse, *Phys. Rev. D* **81**, 123530 (2010).
- [6] J. Preskill, M. B. Wise and F. Wilczek, Cosmology of the invisible axion, *Phys. Lett. B* **120**, 127 (1983).
- [7] L. F. Abbott and P. Sikivie, A cosmological Bbound on the invisible axion, *Phys. Lett. B* **120**, 133 (1983).
- [8] M. Dine and W. Fischler, The not so harmless axion, *Phys. Lett. B* **120**, 137 (1983).
- [9] M. Gorghetto, E. Hardy and G. Villadoro, More axions from strings, *SciPost Phys.* **10**, 050 (2021).
- [10] R. T. Co, L. J. Hall and K. Harigaya, Axion kinetic misalignment mechanism, *Phys. Rev. Lett.* **124**, 251802 (2020).
- [11] P. Sikivie and Q. Yang, Bose-Einstein condensation of dark matter axions, *Phys. Rev. Lett.* **103**, 111301 (2009).
- [12] E. Braaten and H. Zhang, Colloquium : The physics of axion stars, *Rev. Mod. Phys.* **91**, 041002 (2019).
- [13] L. Visinelli, Boson stars and oscillatons: A review, *Int. J. Mod. Phys. D* **30**, 2130006 (2021).
- [14] H. Y. Zhang, Unified view of scalar and vector dark matter solitons, [arXiv:2406.05031](https://arxiv.org/abs/2406.05031).
- [15] M. E. Brown, C. Trujillo and D. Rabinowitz, Discovery of a candidate inner Oort cloud planetoid, *Astrophys. J.* **617**, 589 (2004).
- [16] C. Trujillo, and S. S. Sheppard, A Sedna-like body with a perihelion of 80 astronomical units, *Nature* **507**, 471 (2014).
- [17] K. Batygin and M. E. Brown, Evidence for a distant giant planet in the solar system, *Astron. J.* **151**, 22 (2016).
- [18] P. Mroz, A. Udalski, J. Skowron, R. Poleski, S. Kozłowski, M. K. Szymanski, I. Soszynski, L. Wyrzykowski, P. Pietrukowicz and K. Ulaczyk, *et al.* No large population of unbound or wide-orbit Jupiter-mass planets, *Nature* **548**, 183 (2017).
- [19] H. Niikura, M. Takada, S. Yokoyama, T. Sumi and S. Masaki, Constraints on Earth-mass primordial black holes from OGLE 5-year microlensing events, *Phys. Rev. D* **99**, 083503 (2019).
- [20] S. Sugiyama, M. Takada and A. Kusenko, Possible evidence of axion stars in HSC and OGLE microlensing events, *Phys. Lett. B* **840**, 137891 (2023).
- [21] K. Batygin, F. C. Adams, M. E. Brown, J. C. Becker, The planet nine hypothesis, *Phys. Rep.* **805**, 1 (2019).
- [22] J. Scholtz and J. Unwin, What if planet 9 is a primordial black hole?, *Phys. Rev. Lett.* **125**, 051103 (2020).
- [23] H. Di and H. Shi, Can planet 9 be an axion star?, *Phys. Rev. D* **108**, 103038 (2023).
- [24] H. Di, Stimulated decay of collapsing axion stars and fast radio bursts, *Eur. Phys. J. C* **84**, 283 (2024).
- [25] H. Di, L. Shao, Z. Yi and S. B. Kong, Novel standard candle: Collapsing axion stars, *Phys. Rev. D* **110**, 103031 (2024).
- [26] A. Arza and P. Sikivie, Production and detection of an axion dark matter echo, *Phys. Rev. Lett.* **123**, 131804 (2019).
- [27] A. Arza and E. Todarello, Axion dark matter echo: A detailed analysis, *Phys. Rev. D* **105**, 023023 (2022).
- [28] A. Arza, A. Kryemadhi and K. Zioutas, Searching for axion streams with the echo method, *Phys. Rev. D* **108**, 083001 (2023).
- [29] A. Arza, Q. Guo, L. Wu, Q. Yang, X. Yang, Q. Yuan and B. Zhu, Listening for echo from the stimulated axion decay with the 21 centimeter array, *Sci. Bull.* **69**, 2971 (2024).
- [30] Y. Gong, X. Liu, L. Wu, Q. Yang and B. Zhu, Detecting quadratically coupled ultralight dark matter with stimulated annihilation, *Phys. Rev. D* **109**, 055026 (2024).
- [31] T. W. Kephart and T. J. Weiler, Stimulated radiation from axion cluster evolution, *Phys. Rev. D* **52**, 3226 (1995).
- [32] J. G. Rosa and T. W. Kephart, Stimulated axion decay in superradiant clouds around primordial black holes, *Phys. Rev. Lett.* **120**, 231102 (2018).
- [33] A. Caputo, M. Regis, M. Taoso and S. J. Witte, Detecting the stimulated decay of axions at radio frequencies, *J. Cosmol. Astropart. Phys.* **03** (2019) 027.
- [34] H. Di, H. Shi and Z. Yi, Detection of dilute axion stars with stimulated decay, [arXiv:2407.08436](https://arxiv.org/abs/2407.08436).
- [35] P. Di Vecchia and G. Veneziano, Chiral dynamics in the large n limit, *Nucl. Phys. B* **171**, 253 (1980).
- [36] G. Grilli di Cortona, E. Hardy, J. Pardo Vega and G. Villadoro, The QCD axion, precisely, *J. High Energy Phys.* **01** (2016) 034.
- [37] K. Fujikura, M. P. Hertzberg, E. D. Schiappacasse and M. Yamaguchi, Microlensing constraints on axion stars including finite lens and source size effects, *Phys. Rev. D* **104**, 123012 (2021).
- [38] P. H. Chavanis, Phase transitions between dilute and dense axion stars, *Phys. Rev. D* **98**, 023009 (2018).
- [39] L. Visinelli, S. Baum, J. Redondo, K. Freese and F. Wilczek, Dilute and dense axion stars, *Phys. Lett. B* **777**, 64 (2018).
- [40] J. Eby, M. Leembruggen, L. Street, P. Suranyi and L. C. R. Wijewardhana, Global view of QCD axion stars, *Phys. Rev. D* **100**, 063002 (2019).
- [41] E. Seidel and W. M. Suen, Oscillating soliton stars, *Phys. Rev. Lett.* **66**, 1659 (1991).
- [42] M. P. Hertzberg, Quantum radiation of oscillons, *Phys. Rev. D* **82**, 045022 (2010).
- [43] J. Eby, P. Suranyi and L. C. R. Wijewardhana, The lifetime of axion stars, *Mod. Phys. Lett. A* **31**, 1650090 (2016).
- [44] Z. Wang, L. Shao and L. X. Li, Resonant instability of axionic dark matter clumps, *J. Cosmol. Astropart. Phys.* **07** (2020) 038.
- [45] P. H. Chavanis, Mass-radius relation of Newtonian self-gravitating Bose-Einstein condensates with short-range interactions: I. Analytical results, *Phys. Rev. D* **84**, 043531 (2011).
- [46] P. H. Chavanis and L. Delfini, Mass-radius relation of Newtonian self-gravitating Bose-Einstein condensates with short-range interactions: II. Numerical results, *Phys. Rev. D* **84**, 043532 (2011).
- [47] B. C. Mundim, A numerical study of boson star binaries, [arXiv:1003.0239](https://arxiv.org/abs/1003.0239).
- [48] E. Cotner, Collisional interactions between self-interacting nonrelativistic boson stars: Effective potential analysis and numerical simulations, *Phys. Rev. D* **94**, 063503 (2016).
- [49] B. Schwabe, J. C. Niemeyer and J. F. Engels, Simulations of solitonic core mergers in ultralight axion dark matter

- cosmologies, *Phys. Rev. D* **94**, 043513 (2016).
- [50] J. Eby, M. Leembruggen, J. Leeney, P. Suranyi and L. C. R. Wijewardhana, Collisions of dark matter axion stars with astrophysical sources, *J. High Energy Phys.* **04** (2017) 099.
- [51] M. P. Hertzberg, Y. Li and E. D. Schiappacasse, Merger of dark matter axion clumps and resonant photon emission, *J. Cosmol. Astropart. Phys.* **07** (2020) 067.
- [52] X. Du, D. J. E. Marsh, M. Escudero, A. Benson, D. Blas, C. K. Pooni and M. Fairbairn, Soliton merger rates and enhanced axion dark matter decay, *Phys. Rev. D* **109**, 043019 (2024).
- [53] D. Maseizik and G. Sigl, Distributions and collision rates of ALP stars in the Milky Way, *Phys. Rev. D* **110**, 083015 (2024).
- [54] J. Chen, X. Du, E. W. Lentz, D. J. E. Marsh and J. C. Niemeyer, New insights into the formation and growth of boson stars in dark matter halos, *Phys. Rev. D* **104**, 083022 (2021).
- [55] J. H. H. Chan, S. Sibiryakov and W. Xue, Condensation and evaporation of boson stars, *J. High Energy Phys.* **01** (2024) 071.
- [56] A. S. Dmitriev, D. G. Levkov, A. G. Panin and I. I. Tkachev, Self-similar growth of bose stars, *Phys. Rev. Lett.* **132**, 091001 (2024).
- [57] D. G. Levkov, A. G. Panin and I. I. Tkachev, Relativistic axions from collapsing Bose stars, *Phys. Rev. Lett.* **118**, 011301 (2017).
- [58] J. Eby, M. Leembruggen, P. Suranyi and L. C. R. Wijewardhana, Collapse of axion stars, *J. High Energy Phys.* **12** (2016) 066.
- [59] P. J. Fox, N. Weiner and H. Xiao, Recurrent axion stars collapse with dark radiation emission and their cosmological constraints, *Phys. Rev. D* **108**, 095043 (2023).
- [60] L. Caloni, M. Gerbino, M. Lattanzi and L. Visinelli, Novel cosmological bounds on thermally-produced axion-like particles, *J. Cosmol. Astropart. Phys.* **09** (2022) 021.
- [61] R. Balkin, J. Serra, K. Springmann, S. Stelzl and A. Weiler, White dwarfs as a probe of exceptionally light QCD axions, *Phys. Rev. D* **109**, 095032 (2024).
- [62] A. Gómez-Bañón, K. Bartnick, K. Springmann and J. A. Pons, Constraining light QCD axions with isolated neutron star cooling, [arXiv:2408.07740](https://arxiv.org/abs/2408.07740).
- [63] D. R. Lorimer, M. Bailes, M. A. McLaughlin, D. J. Narkevic, and F. Crawford A bright millisecond radio burst of extragalactic origin, *Science*, **318**, 777 (2007).
- [64] E. F. Keane, B. W. Stappers, M. Kramer and A. G. Lyne, On the origin of a highly-dispersed coherent radio burst, *Mon. Not. Roy. Astron. Soc.* **425**, 71 (2012).
- [65] D. Thornton, B. Stappers, M. Bailes, B. R. Barsdell, S. D. Bates, N. D. R. Bhat, M. Burgay, S. Burke-Spolaor, D. J. Champion and P. Coster, *et al.* A population of fast radio bursts at cosmological distances, *Science* **341**, 53 (2013).
- [66] E. Petroff, J. W. T. Hessels and D. R. Lorimer, Fast radio bursts, *Astron. Astrophys. Rev.* **27**, 4 (2019).
- [67] L. G. Spitler, J. M. Cordes, J. W. T. Hessels, D. R. Lorimer, M. A. McLaughlin, S. Chatterjee, F. Crawford, J. S. Deneva, V. M. Kaspi and R. S. Wharton, *et al.* Fast radio burst discovered in the arecibo pulsar ALFA survey, *Astrophys. J.* **790**, 101 (2014).
- [68] C. J. Hogan and M. J. Rees, Axion miniclusters, *Phys. Lett. B* **205**, 228 (1988).
- [69] E. W. Kolb and I. I. Tkachev, Axion miniclusters and bose stars, *Phys. Rev. Lett.* **71**, 3051 (1993).
- [70] E. W. Kolb and I. I. Tkachev, Femtolensing and picolensing by axion miniclusters, *Astrophys. J. Lett.* **460**, L25 (1996).
- [71] B. Eggemeier, J. Redondo, K. Dolag, J. C. Niemeyer and A. Vaquero, First simulations of axion minicluster halos, *Phys. Rev. Lett.* **125**, 041301 (2020).
- [72] J. I. Read, The local dark matter density, *J. Phys. G* **41**, 063101 (2014).
- [73] P. J. McMillan, The mass distribution and gravitational potential of the Milky Way, *Mon. Not. Roy. Astron. Soc.* **465**, 76 (2016).
- [74] N. W. Evans, C. A. J. O'Hare and C. McCabe, Refinement of the standard halo model for dark matter searches in light of the Gaia Sausage, *Phys. Rev. D* **99**, 023012 (2019).
- [75] P. F. de Salas and A. Widmark, Dark matter local density determination: recent observations and future prospects, *Rept. Prog. Phys.* **84**, 104901 (2021).
- [76] L. Sun et al., "Compact, Stable, Repetitive GW-Level S-Band Multibeam Relativistic Klystron Amplifier Operating Over a Longer Period in a Lower Magnetic Field," *IEEE Trans. Electron Devices* **70**, 6571 (2023).